catalysts

Article

Sulfadiazine Elimination from Wastewater Effluents under Ozone-Based Catalysis Processes

Ruixue Li [1], Yanqiong Zhang [1], Fengru Lu [1], Feng Li [1], Lijie Xu [2], Lu Gan [3], Chao Cui [4], Xuesong Li [4], Qiutong Jin [5], Wei Chu [5,*], Muting Yan [1,5,*] and Han Gong [1,*]

[1] Joint Laboratory of Guangdong Province and Hong Kong Region on Marine Bioresource Conservation and Exploitation, College of Marine Sciences, South China Agricultural University, Guangzhou 510642, China; liruixue198@163.com (R.L.); yanqiong222@outlook.com (Y.Z.); lufengru1215@163.com (F.L.); lili425@stu.scau.edu.cn (F.L.)

[2] College of Biology and the Environment, Nanjing Forestry University, Nanjing 210000, China; xulijie@njfu.edu.cn

[3] College of Materials Science and Engineering, Nanjing Forestry University, Nanjing 210000, China; ganlu@njfu.edu.cn

[4] Bureau of Agriculture and Rural Affairs of Pingyi County, Linyi 510000, China; cuichao808@163.com (C.C.); lxs08@163.com (X.L.)

[5] Department of Civil and Environmental Engineering, The Hong Kong Polytechnic University, Hong Kong 999077, China; 13160662815@163.com

* Correspondence: cewchu@polyu.edu.hk (W.C.); marineymt@scau.edu.cn (M.Y.); han.gong@connect.polyu.hk or gonghan@scau.edu.cn (H.G.)

Abstract: The presence of antibiotic sulfadiazine (SFD) poses threats to the ecosystem and human health, and traditional wastewater treatment processes are not ideal for sulfadiazine removal. Therefore, it is urgent to develop treatment processes with high efficiency targeting sulfadiazine. This study investigated the degradation and mineralization mechanisms of SFD by ozone-based catalysis processes including ozone/persulfate (PS) and ozone/peroxymonosulfate (PMS). The degradation, mineralization and byproducts of SFD were monitored by HPLC, TOC and LC/MS, respectively. SFD was efficiently removed by two ozone-based catalysis processes. Ozone/PMS showed high efficiency for SFD removal of 97.5% after treatment for 1 min and TOC reduction of 29.4% after treatment for 20 min from wastewater effluents. SFD degradation was affected by pH, oxidant dosage, SFD concentration and anions. In the two ozone-based catalysis processes, hydroxyl radicals (OH•) and sulfate radicals (SO_4•$^-$) contributed to the degradation of SFD. The degradation pathways of SFD under the two processes included hydroxylation, the opening of the pyrimidine ring and SO_2 extrusion. The results of this study demonstrate that the two ozone-based catalysis processes have good potential for the elimination of antibiotics from water/wastewater effluents.

Keywords: sulfadiazine; ozone; persulfate; peroxymonosulfate; catalysis

Citation: Li, R.; Zhang, Y.; Lu, F.; Li, F.; Xu, L.; Gan, L.; Cui, C.; Li, X.; Jin, Q.; Chu, W.; et al. Sulfadiazine Elimination from Wastewater Effluents under Ozone-Based Catalysis Processes. *Catalysts* **2023**, *13*, 1076. https://doi.org/10.3390/catal13071076

Academic Editors: Hao Xu and Yanbiao Liu

Received: 29 May 2023
Revised: 3 July 2023
Accepted: 3 July 2023
Published: 6 July 2023

1. Introduction

Emerging contaminants such as pharmaceuticals, pesticides and personal care products are frequently detected in water bodies including municipal wastewater, surface water and drinking water sources, posing threats to the environment and human health [1–4]. Antibiotics are an important group of pharmaceuticals that are commonly detected in water bodies, soil and so on due to their misuse in human, veterinary and agricultural fields [5–7]. Sulfadiazine (SFD) is an antibiotic that is mostly used with pyrimethamine to treat toxoplasmosis. It can also be used to treat otitis media and prevent rheumatic fever, chancroid, malaria, chlamydia and *Haemophilus influenza* infections [8]. Due to its high antimicrobial activities, broad spectrum and low costs, SFD is commonly applied for medical use for human and animal infections as well as in agricultural feeds [9,10].

Due to incomplete metabolism, approximately 70% of consumed antibiotics are released into the environment and SFD has been frequently detected in sediments, soil and water bodies. For example, approximately 0.019 μg/L of SFD was detected in processed sewage in cities of Canada, whereas in an effluent, after secondary treatment in Germany, the detection level of SFD was 0.081 μg/L [11]. In the surface water of Poyang Lake, China, the maximum concentration of SFD was 0.056 μg/L [12].

It has been reported in previous studies that SFD has negative impacts on various aquatic organisms in the environment. For example, the green algae *Selenastrum capricornutum* has an EC_{50} at 3.43 mg/L (a 50% reduction in growth), the EC_{50} of the water flea *Daphnia magna* is 88.0 mg/L (a 50% reduction in reproductive output) and the rainbow trout *Oncorhynchus mykiss* has an LC_{50} at 103.0 mg/L [13–15]. The presence of antibiotics in the environment can lead to the formation of complex contaminants with heavy metals, persistent organic pollutants such as microplastics and so on, which enhance the toxicity of antibiotics [16,17]. In addition, the long-term persistence of antibiotics in the environment induces the development of antibiotic resistance genes (ARGs) and antibiotic resistance bacteria (ARB), which could be more damaging to the environment and humans than the antibiotics themselves [16,18,19]. It has been revealed that the efficiency of removing antibiotics from traditional water/wastewater treatment plants (WWTPs) is relatively low [20] since traditional methods such as coagulation, adsorption and biodegradation cannot remove antibiotics from wastewater efficiently [21]. Therefore, it is urgent to develop treatment technologies with high removal efficiency targeted toward SFD.

In recent years, advanced oxidation processes (AOPs) have received increasing attention for the removal of antibiotics from the environment. AOPs include ionizing radiation, Fenton and Fenton-like reactions, ozonation, photocatalytic oxidation, and electrochemical oxidation [22–24]. Previous studies have demonstrated that AOPs are effective not only for antibiotic removal but also for ARB inactivation and ARGs removal [22,25]. Due to their advantages of stability, nontoxicity, low cost and environmental friendliness, oxidants such as peroxymonosulfate (PMS)- and persulfate (PS)-based AOPs for micropollutant removal have attracted increasing attention [26–28]. Antibiotics and other drugs can be directly oxidatively removed by PMS and PS; nevertheless, their reaction rate is very low [29–32]. PMS and PS can be activated by photocatalysts, heating and metal ions to produce highly reactive oxygen species (ROS) such as hydroxyl radicals (•OH) and sulfate radicals ($SO_4•^-$) [26,33–37]. According to Feng et al. (2017), the catalysis process PMS/Fe (VI) promoted the generation of $SO_4•^-$ and •OH and enhanced the degradation of fluoroquinolones (FQ) [38].

Ozone is a commonly used oxidant in water treatment, with an oxidation-reduction potential of 2.07 V and 1.24 V for acidic and alkaline solutions, respectively. Previous studies showed that although ozone can remove antibiotics from water, the removal efficiency was relatively low [39]. Removal efficiency can be improved by combining ozonation with other disinfectors, e.g., PMS (HSO_5^-) or PS ($S_2O_8^{2-}$), which have received great attention in wastewater purification because of their ability to produce $SO_4•^-$ [31,40]. Previous studies showed that 1,4-dioxane, chloramphenicol, sulfamethoxazole and trimethoprim were efficiently removed by processes using ozone/PMS and ozone/PS [41–43]. In this study, ozone-based catalysis processes using ozone/PMS and ozone/PS were performed to examine the potential of combined processes in SFD removal. The degradation rate of SFD by ozonation and the combined processes were compared, and the effects of reaction parameters and environmental factors including dosages of oxidants, initial concentrations of SFD, pH and inorganic anions on SFD degradation were examined. The application of combined processes in real wastewater was performed and the reaction mechanisms of SFD degradation in the ozone-based catalysis processes were revealed.

2. Results and Discussion

2.1. Degradation Performance of Different Oxidation Processes

The degradation of SFD under different oxidation processes is shown in Figure 1. The sole PS and sole PMS processes showed negligible removal of SFD, with degradation efficiencies of only 3.9% and 5.9% within 10 min, respectively. The sole ozone process removed only 23.8% of the SFD in 10 min. When ozone was involved in the reaction with PS or PMS, the SFD degradation efficiency increased significantly, reaching 64.6% and 73.7% within 10 min, respectively. This may have been due to the catalysis of PS and PMS by ozone to produce reactive oxygen species (ROS) such as •OH and $SO_4\bullet^-$ that could remove the target contaminants [1,2,44,45]. At the same concentration and removal time, the ozone/PMS process had higher removal efficiency than the ozone/PS process. This can likely be attributed to the fact that PMS has an asymmetric structure and long superoxide bonds (O–O), which are more easily activated [36,46].

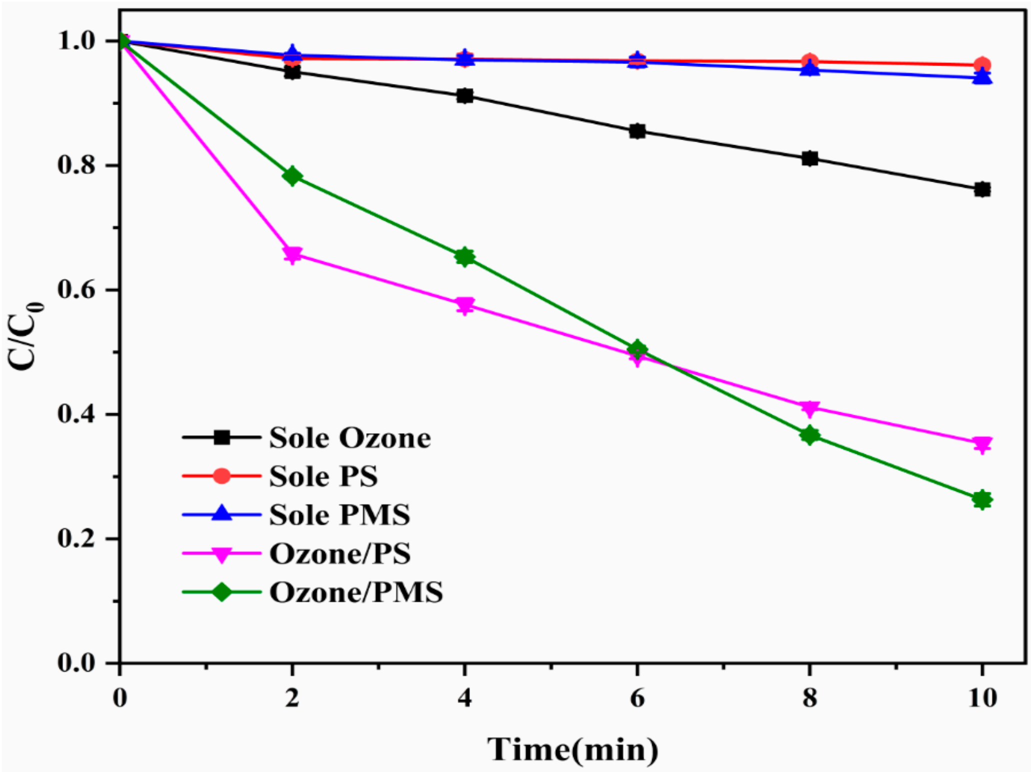

Figure 1. SFD degradation under different treatment processes. Experiment conditions: [SFD] = 0.03 mM, [ozone flow rate] = 2.14 g/min, [PS] = 1.5 mM, [PMS] = 1.5 mM, pH = 8.0.

In addition, the degradation efficiency of SFD from previously reported literature is summarized in Table 1 for comparison. It was worth noting that the rate constant (k) of SFD removal from the wastewater effluent in the ozone/PMS process was higher than that for other processes, which fully illustrated that the ozone/PMS process was an efficient degradation method for SFD.

Table 1. Comparison of different advanced oxidation processes for degradation of SFD.

Processes	Reaction Conditions	SFD	Matrix	Removal Rate	k (min^{-1})	Refs.
Co_3O_4-MnO_2/BC/PMS	[catalyst] = 0.1 g/L [PMS] = 1 mM pH = 7.0	25 mg/L	Ultrapure water	100% (10 min)	0.482	[47]
ZIF-CoN_3P-C/PMS	[catalyst] = 0.05 g/L [PMS] = 1 mM pH = 3.35	10 mg/L	Ultrapure water	98.4% (5 min)	1.074	[48]

Table 1. *Cont.*

Processes	Reaction Conditions	SFD	Matrix	Removal Rate	k (min^{-1})	Refs.
$Fe_3O_4@Co_3S_4$-3/PMS	[catalyst] = 0.2 g/L [PMS] = 1 mM pH = 6.9	20 mg/L	Ultrapure water	95% (2 min)	1.1609	[49]
S-Fe^0/PMS	[catalyst] = 0.05 g/L [PMS] = 0.5 mM pH = 5.4	0.08 mM	Ultrapure water	99.4% (60 min)	0.296	[50]
MBC/PS	[catalyst] = 1.0 mg/L [PS] = 1.5 mM pH = 5.16	40 mg/L	Ultrapure water	91.79% (60 min)	0.0309	[51]
Two-stage US-ZVI/PS	[US power] = 90 W [catalyst] = 0.6 mM [PS] = 1.4 mM pH = 6.5	20 mg/L	Ultrapure water	97.4% (15 min)	0.279	[52]
UV/Oxone	[UV intensity] = 0.272 mW/cm^2 [Oxone] = 80 µM pH = 7.0	20 µM	Ultrapure water	98.9% (10 min)	0.4518	[53]
Ozone/PS	[Ozone flow rate] = 2.14 g/min [PS] = 3.0 mM pH = 8.0	0.03 mM	Ultrapure water	96.5% (20 min)	0.163	This work
			Effluent	91.8% (20 min)	0.1315	
Ozone/PMS	[Ozone flow rate] = 2.14 g/min [PMS] = 3.0 mM pH = 8.0	0.03 mM	Ultrapure water	99.3% (20 min)	0.2267	This work
			Effluent	97.5% (1 min)	3.579	

2.2. Influence of Reaction Parameters

2.2.1. Effects of Initial SFD Concentrations and Oxidant Dosages

As shown in Figure 2, the degradation rate of SFD gradually decreased with the increase of the initial concentration of SFD under the two ozone-based catalysis processes ozone/PS and ozone/PMS. This can be attributed to the fact that the active species produced in the system were constant, and the higher the initial concentration of SFD, the less radicals were shared [54]. Figure 3 shows the effect of the oxidant dosage on SFD degradation. For the process using ozone/PMS, the degradation efficiency increased from 47.5% to 99.5% in the range of 0 mM to 3.0 mM. For the process using ozone/PS, the removal efficiency of SFD increased from 47.5% at 0 mM to 79.9% at 3.0 mM with the increase in PS concentration. Moreover, the reaction rate constant gradually increased as the oxidant dosage increased (Figure 3b). As the oxidant dosages increased, the $SO_4\bullet^-$ and $\bullet OH$ radicals generated by PMS and PS also increased (Equations (1)–(11)) [2,31,40,55–60], which may have led to a higher degradation rate.

$$SO_5^{2-}\ (PMS) + O_3 \rightarrow SO_8^{2-} \quad k = (2.12 \pm 0.03) \times 10^4\ M^{-1}\ s^{-1} \tag{1}$$

$$SO_8^{2-} \rightarrow SO_5\bullet^- + O_3\bullet^- \tag{2}$$

$$SO_5\bullet^- + O_3 \rightarrow SO_4\bullet^- + 2O_2 \quad k = 1.6 \times 10^5\ M^{-1}\ s^{-1} \tag{3}$$

$$SO_5\bullet^- + H_2O \rightarrow SO_4\bullet^- + \bullet OH \tag{4}$$

$$SO_5\bullet^- + SO_5\bullet^- \rightarrow 2\ SO_4\bullet^- + O_2 \quad k = 2.1 \times 10^8\ M^{-1}\ s^{-1} \tag{5}$$

$$O_3\bullet^- \rightarrow O\bullet^- + O_2 \tag{6}$$

$$O\bullet^- + H_2O \rightarrow \bullet OH + OH^- \tag{7}$$

$$S_2O_8^{2-}\ (PS) + H_2O \rightarrow HO_2^- + 2SO_4^{2-} + 3H^+ \tag{8}$$

$$S_2O_8^{2-} + HO_2^- \rightarrow SO_4\bullet^- + SO_4^{2-} + H^+ + \bullet O_2^- \tag{9}$$

$$O_3 + OH^- \rightarrow HO_2^- + O_2 \quad k = 70\ M^{-1}\ s^{-1} \tag{10}$$

$$O_3 + HO_2^- \rightarrow \bullet OH + \bullet O_2^- + O_2 \quad k = 2.8 \times 10^6\ M^{-1}\ s^{-1} \tag{11}$$

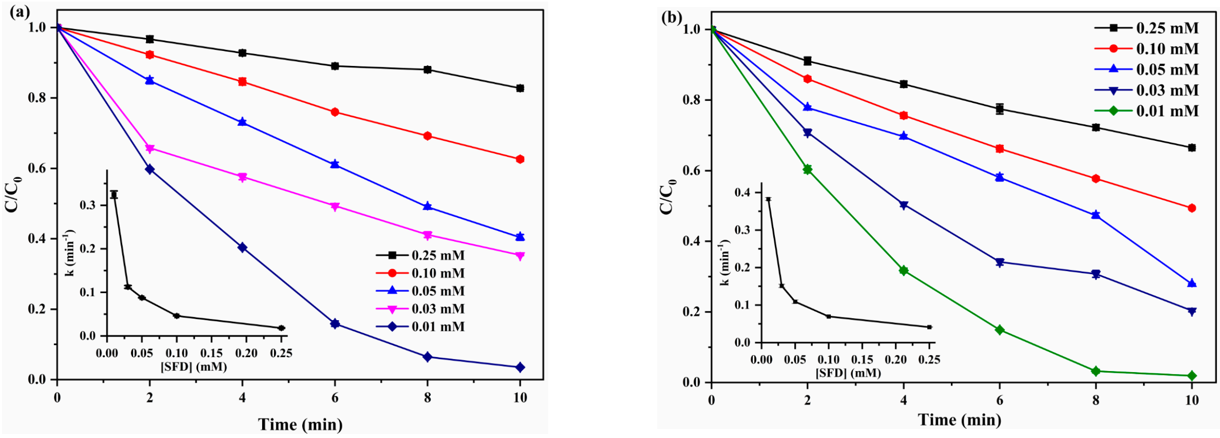

Figure 2. Effect of initial SFD concentration on SFD degradation rate in different processes. (**a**) Ozone/PS system. (**b**) Ozone/PMS system. Experiment conditions: [PS] = 1.5 mM, [PMS] = 1.5 mM, [ozone flow rate] = 2.14 g/min, pH = 8.0.

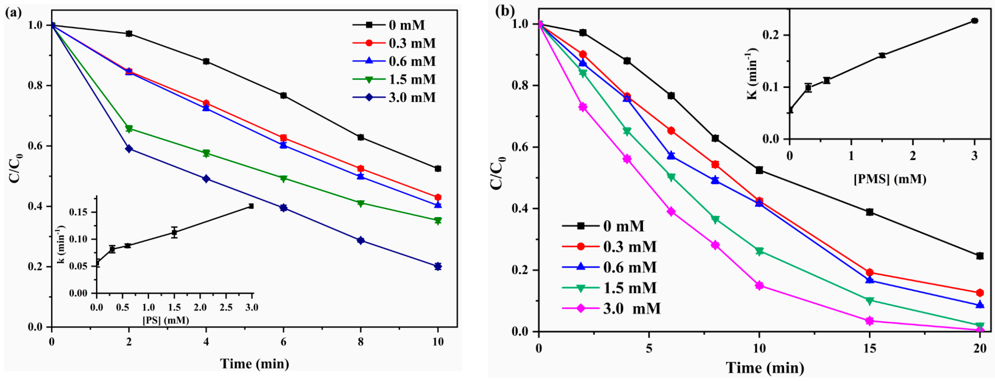

Figure 3. Effect of oxidant dosages on SFD degradation by (**a**) Ozone/PS system and (**b**) Ozone/PMS system. Experiment conditions: [ozone flow rate] = 2.14 g/min, [SFD]= 0.03 mM, pH = 8.0.

2.2.2. Effect of Initial pH

The influence of pH on SFD degradation was evaluated in the pH range of 3.5 to 9.5 (Figure 4). As shown in Figure 4a, the ozone/PS process removed SFD with the optimal degradation at an initial pH of 9.5, with a total removal rate of 99.4% at the end of the reaction (20 min) and a decay rate constant of 0.27 min^{-1}. The final removal rate of SFD had no clear difference within the pH range of 5.0 to 8.0. At the initial pH of 3.5, the removal rate of SFD was the lowest with the ozone/PS treatment process. PS was converted into $HS_2O_8^-$ (Equation (12)) and the $SO_4\bullet^-$ radicals were consumed by excessive hydrogen ions (H^+) (Equation (13)), resulting in a decrease in $SO_4\bullet^-$ under extremely acidic conditions (pH = 3.0) [61]. On the contrary, in the alkaline environment, OH^- in the solution could directly activate PS to produce $SO_4\bullet^-$ and $\bullet OH$ through the hydrolysis of PS (Equations (14)–(17)) [40,43,62].

$$S_2O_8{}^{2-} + H^+ \rightarrow HS_2O_8{}^- \quad (12)$$

$$SO_4\bullet^- + SO_4{}^{2-} + H^+ \rightarrow HS_2O_8{}^- \quad (13)$$

$$S_2O_8{}^{2-} + H_2O \rightarrow SO_5{}^{2-} + SO_4{}^{2-} + 2H^+ \quad (14)$$

$$SO_5{}^{2-} + H_2O \rightarrow HO_2{}^- + SO_4{}^{2-} + H^+ \quad (15)$$

$$HO_2{}^- + S_2O_8{}^{2-} \rightarrow SO_4\bullet^- + SO_4{}^{2-} + H^+ + \bullet O_2{}^- \quad (16)$$

$$SO_4\bullet^- + OH^- \rightarrow SO_4{}^{2-} + \bullet OH \ k = 6.5 \times 10^7 \ M^{-1} \ s^{-1} \quad (17)$$

For the ozone/PMS process, at the initial pH range of 3.5 to 9.5, the SFD removal efficiencies were above 99.0% at the end of the reaction (20 min) and did not change significantly (Figure 4b). Similar results have been reported. For example, the effect of the initial pH solution was negligible on ofloxacin degradation by a PMS/perovskite catalysis process, according to Gao et al. [34]. The high efficiency of SFD degradation can be attributed to the role of $SO_4\bullet^-$ and •OH in the degradation. The radical •OH can play a role in degradation in the pH range of 5.0 to 11.0. When the pH was 7.0, $SO_4\bullet^-$ and •OH had the same influence on the degradation of organic pollutants [63]. However, $SO_4\bullet^-$ radicals play a key role in the removal of contaminants at a pH below 7.0 [63,64]. As the degradation of SFD is not significantly dependent on pH, the ozone/PMS process can be applied in water/wastewater treatment under a wide range of pH levels.

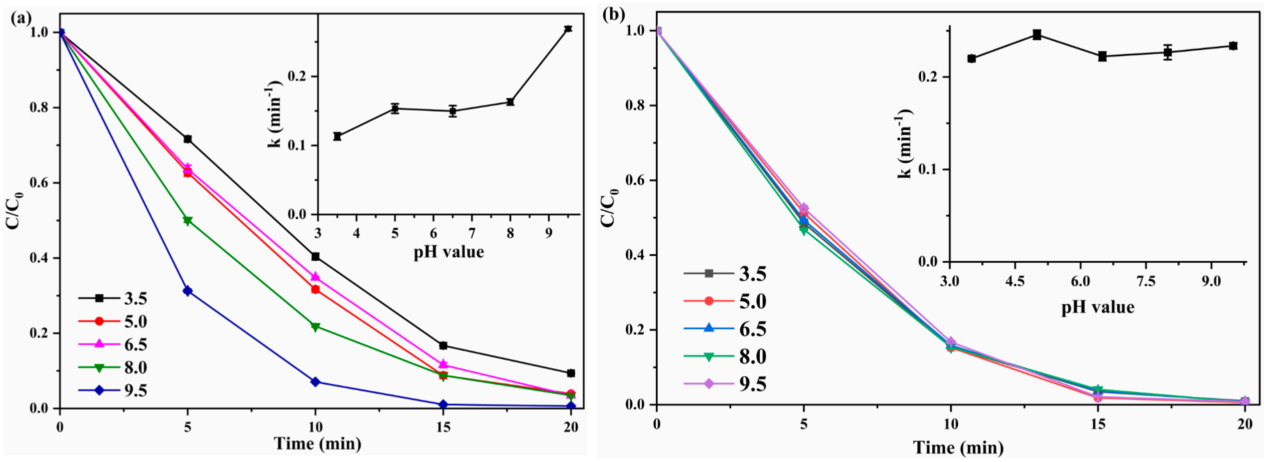

Figure 4. Effect of initial pH on SFD degradation by the (**a**) ozone/PS process and (**b**) ozone/PMS process. Experiment conditions: [SFD] = 0.03 mM, [PS] = 3.0 mM, [PMS] = 3.0 mM, [ozone flow rate] = 2.14 g/min.

2.3. Influence of Water Matrix

To further understand the degradation efficiency of SFD in real wastewater, three treatment processes including ozone, ozone/PS and ozone/PMS were compared for the degradation of SFD in ultrapure water and wastewater effluent matrices (Figure 5). Similarly, in the wastewater effluents, the degradation efficiency of SFD by different processes was in the order of ozone/PMS > ozone/PS > ozone (Figure 5a). The removal efficiency of SFD by the ozone/PS process was 91.8% and 96.5% for the wastewater effluents and ultrapure water, respectively. Compared to the ultrapure water, the sole ozone and ozone/PMS processes showed higher degradation rates of SFD in the wastewater effluents. Moreover, SFD removal was much faster in wastewater effluents (with approximately 97.5% removal efficiency after treatment for 1 min) compared to ultrapure water under the ozone/PMS process. Wang et al. (2018) documented that polymeric carbon nitride foam could remove tetracycline antibiotics under visible light and achieved the highest removal rate of 78.9% in natural seawater, followed by reservoir water (75.0%), tap water (62.3%), deionized water (49.8%), reverse osmosis concentrate (32.7%) and pharmaceutical wastewater (18.9%) [65]. SFD removal in the wastewater effluents was slightly lower than that in the ultrapure water under the catalysis process ozone/PS. The differences in the removal rates of the contaminants in different water matrices may be due to a combination of factors such as solution pH, inorganic ion species, dissolved organic matter and so on [30,65,66].

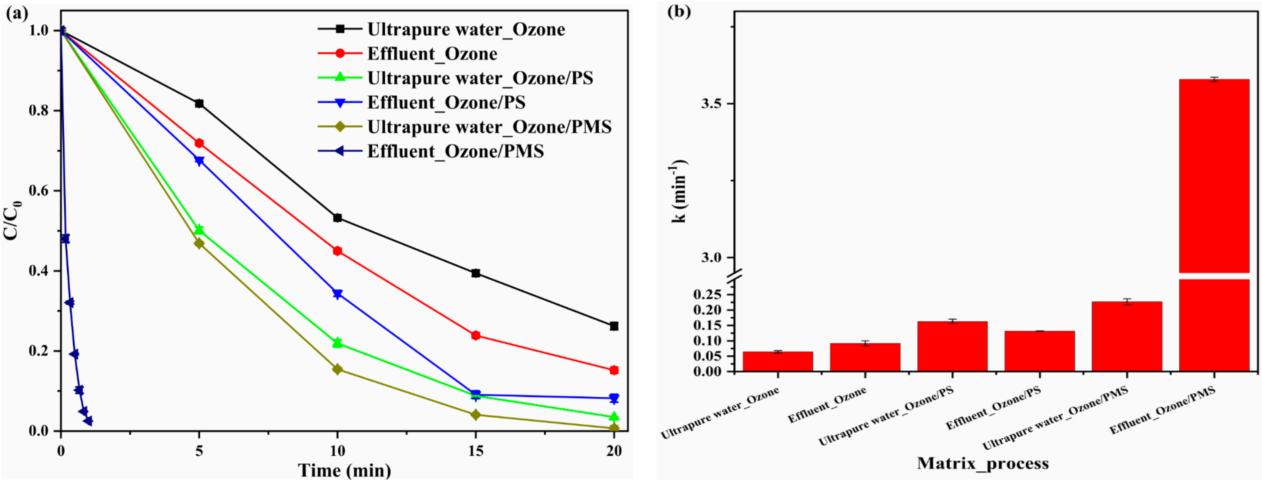

Figure 5. SFD degradation in effluent matrices. (**a**) Decay curves. (**b**) Reaction rate constants. Experiment conditions: [SFD] = 0.03 mM, [PS] = 3.0 mM, [PMS] = 3.0 mM, [ozone flow rate] = 2.14 g/min.

2.4. Influence of Anions on SFD Degradation

Some common anions including sulfate (SO_4^{2-}), phosphate (PO_4^{3-}), bromide (Br^-), chloride (Cl^-), nitrate (NO_3^-) and nitrite (NO_2^-) may affect the degradation of SFD. Therefore, the removal of SFD by the ozone/PS and ozone/PMS processes was investigated in the presence of different anions (Figure 6). The anion levels applied in this study were based on those determined for the wastewater effluents.

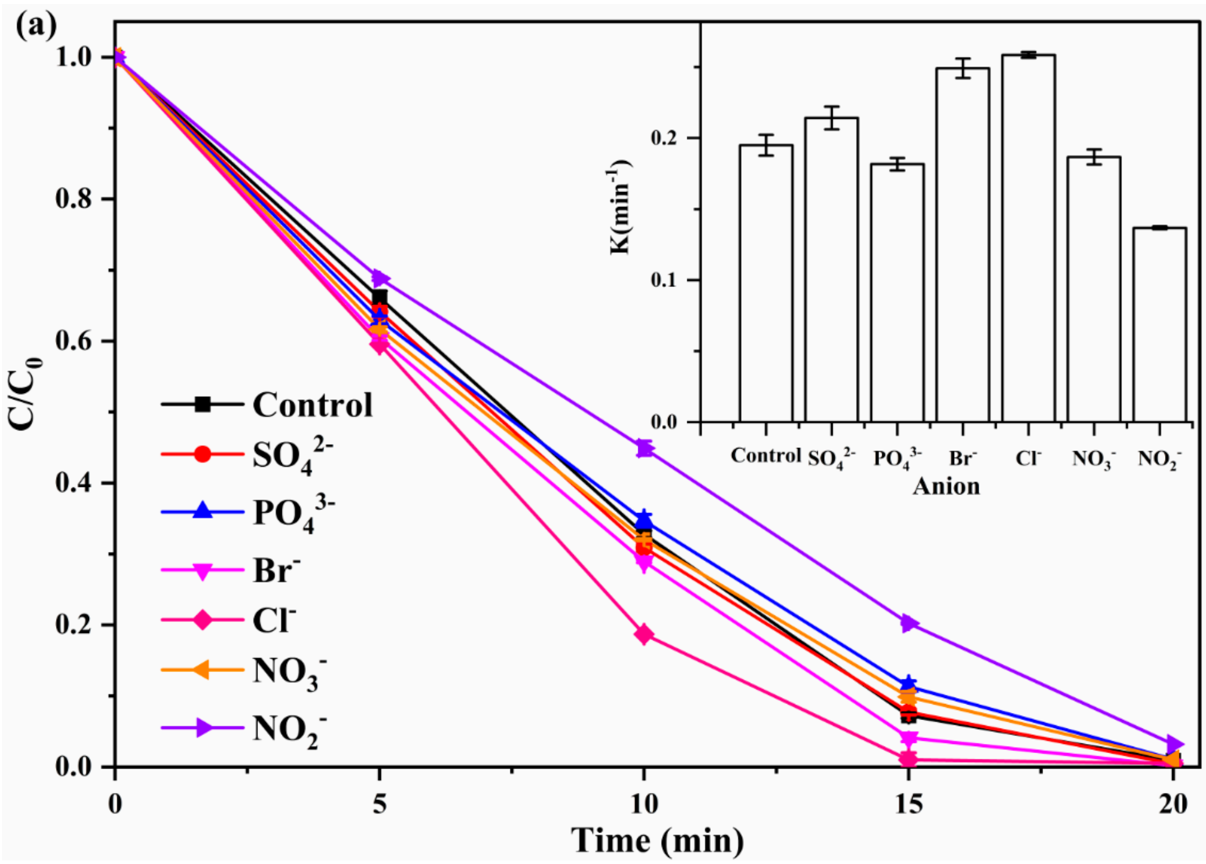

Figure 6. *Cont.*

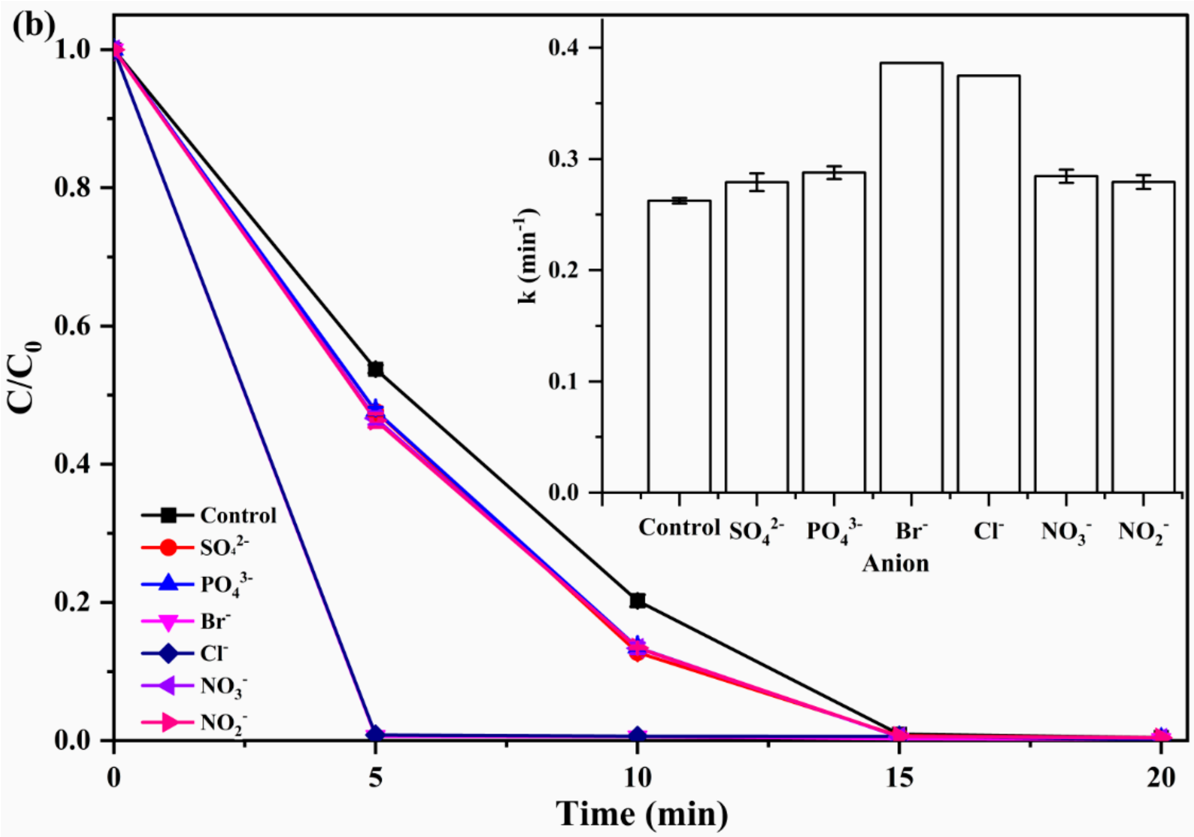

Figure 6. (**a**) Effect of anions on SFD degradation by the ozone/PS process. (**b**) Effect of anions on SFD degradation by the ozone/PMS process. Experiment conditions: [SFD] = 0.03 mM, [ozone flow rate] = 3.21 g/min, [PS] = 3.0 mM, [PMS] = 3.0 mM, [SO_4^{2-}] = 5.915 mM, [PO_4^{3-}] = 0.002 mM, [Br^-] = 0.166 mM, [Cl^-] = 105.63 mM, [NO_3^-] = 0.002 mM, [NO_2^-] = 0.024 mM.

As shown in Figure 6a, in the ozone/PS treatment process, the decay rate constant of SFD increased from 0.20 min^{-1} to 0.26 min^{-1} in the presence of Cl^-. This may have been due to the reaction of Cl^- with $SO_4\bullet^-$ to generate halogen radicals ($Cl\bullet$ or $Cl_2\bullet$), which are more selective than $SO_4\bullet^-$ in degrading electron-rich compounds (Equation (18)) [67,68]. When Br^- was present, the decay rate constant of SFD increased to 0.25 min^{-1}. As reported by Zhang et al. (2020), the degradation of sulfamethoxazole by UV/PS was also slightly promoted in the presence of Br^- within 5 min [69]. This may have been due to the fact that the influence of Br^- on the removal of organic matter is not only related to the conversion of Br^- but also to the properties of the organic matter itself [69]. In addition, the slight promotion of SFD degradation by ozone/PS was also found in the presence of SO_4^{2-}, with pseudo-first-order degradation rate constants of approximately 0.21 min^{-1}. In contrast, the presence of PO_4^{3-}, NO_3^- and NO_2^- inhibited the removal of SFD to different extents. The inhibitory effect of NO_2^- can be explained by its ability to destroy the $\bullet OH$ and $SO_4\bullet^-$ produced in the reaction system as a reducing agent (Equation (19)) [70,71]. The inhibitory effects of PO_4^{3-} and NO_3^- were less notable compared to those of NO_2^-, and their inhibitory effects may be related to their ability to act as bursting agents to scavenge $\bullet OH$ and $SO_4\bullet^-$ radicals [72]. The inhibitory effects of PO_4^{3-}, NO_3^- and NO_2^- possibly explain the slight decrease of SFD removal in the effluent compared to that in the ultrapure water by ozone/PS.

$$SO_4\bullet^- + Cl^- \rightarrow Cl\bullet + SO_4^{2-} \quad k = 2.7 \times 10^8\ M^{-1}\ s^{-1} \tag{18}$$

$$NO_2^- + \bullet OH \text{ or } SO_4\bullet^- \rightarrow NO_2\bullet + HO^- \text{ or } SO_4^{2-} \quad k = 1.0 \times 10^{10} \text{ or } 8.0 \times 10^8\ M^{-1}\ s^{-1} \tag{19}$$

Figure 6b shows the effects of anions on SFD removal under the ozone/PMS treatment process. Compared with the ozone/PS process, the anions in the ozone/PMS process all promoted the degradation of SFD to different degrees. Compared to the control group without anions, the presence of Br^- and Cl^- promoted the degradation of SFD, with the decay rate constant increasing by 0.12 min^{-1} and 0.11 min^{-1}, respectively. The promotion of Cl^- in SFD elimination was mainly attributed to the possible involvement of Cl^- in the decomposition reaction of PMS, and the generated Cl_2 and HOCl could enhance the removal of SFD (Equations (20) and (21)) [73,74]. A possible explanation for the contribution of Br^- to SFD removal is that Br^- can be oxidized by PMS in a formal two-electron process to generate the strong oxidant HOBr (Equations (22) and (23)) [75,76]. SO_4^{2-}, PO_4^{3-}, NO_3^- and NO_2^- slightly promoted the degradation of SFD. The presence of PO_4^{3-} promoted the degradation of SFD, which can be explained by the fact that PO_4^{3-} was also able to effectively activate PMS to generate free radicals to degrade the contaminants [16].

$$Cl^- + HSO_5^- \rightarrow SO_4^{2-} + HOCl \quad (20)$$

$$2Cl^- + HSO_5^- + H^+ \rightarrow SO_4^{2-} + Cl_2 \quad (21)$$

$$HSO_5^- + Br^- \rightarrow SO_4^{2-} + HOBr \ k = 0.7\ M^{-1}\ s^{-1} \quad (22)$$

$$SO_5^{2-} + Br^- \rightarrow SO_4^{2-} + HOBr \ k = 0.17\ M^{-1}\ s^{-1} \quad (23)$$

2.5. TOC Abatement in SFD Degradation

Figure 7 shows the mineralization of SFD in the ozone/PS and ozone/PMS processes. In ultrapure water, the final TOC removal rates of the ozone/PS and ozone/PMS processes were 18.1% and 19.0% after treatment for 20 min, respectively. In the wastewater effluents, the ozone/PMS process showed higher mineralization than the ozone/PS process, with a TOC removal rate of 29.4% compared to 20.1% after 20 min. TOC removal in the wastewater effluents was higher than that in ultrapure water in the two treatment systems. The increase in TOC removal rates may have been due to the more significant degradation of SFD and intermediate products. Except for the direct attack oxidants, there was also the generation of •OH and SO_4•$^-$ radicals, which facilitate the reduction of TOC and the degradation of intermediates.

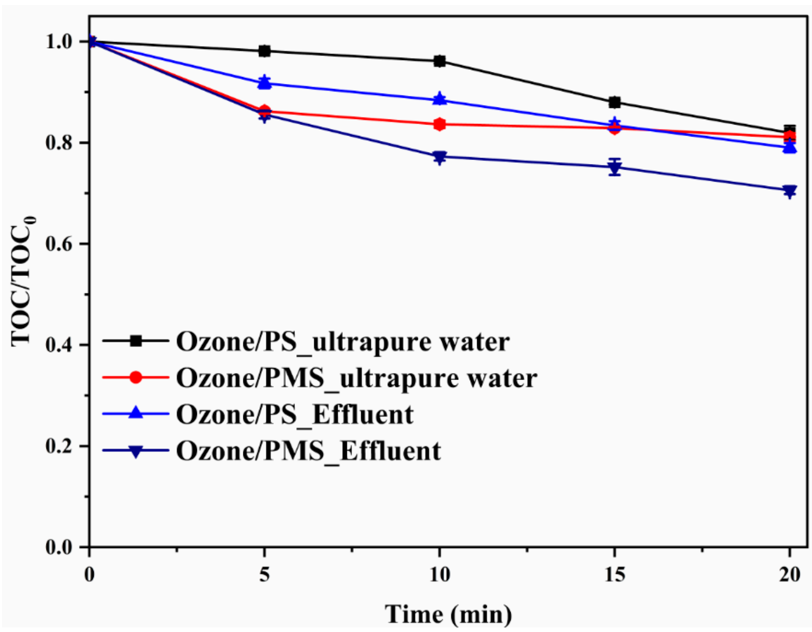

Figure 7. Mineralization of SFD by different processes. Experiment conditions: [SFD] = 0.03 mM, [ozone flow rate] = 3.21 g/min, [PS] = 3.0 mM, [PMS] = 3.0 mM.

2.6. Contributions of Different Reactive Species

To confirm the dominant reactive species in the ozone/PS and ozone/PMS reactions, radical quenching experiments were carried out (Figure 8). TBA was used to scavenge •OH ($k_{•OH\text{-}TBA}$ = 6.0 × 10^8 M^{-1} s^{-1}) [31], while MeOH was highly reactive to both •OH ($k_{•OH\text{-}MeOH}$ = 9.7 × 10^8 M^{-1} s^{-1}) and $SO_4•^-$ ($kSO_4•^-{}_{\text{-}MeOH}$ = 1.0 × 10^7 M^{-1} s^{-1}) [77]. In the ozone/PS process, the SFD removal rate decreased by 5.5% and 23.2% within 10 min when TBA and MeOH were added, respectively, indicating that the removal efficiency of SFD decreased by 5.5% and 17.7% due to the quenching of •OH and $SO_4•^-$ radicals (Figure 8a). Similarly, in the ozone/PMS process, the removal efficiency of SFD decreased by 9.0% and 18.5% due to the quenching of •OH and $SO_4•^-$ radicals, respectively (Figure 8b). The results showed that •OH and $SO_4•^-$ radicals contributed to SFD elimination in the ozone/PS and ozone/PMS processes, and $SO_4•^-$ played a relatively major role.

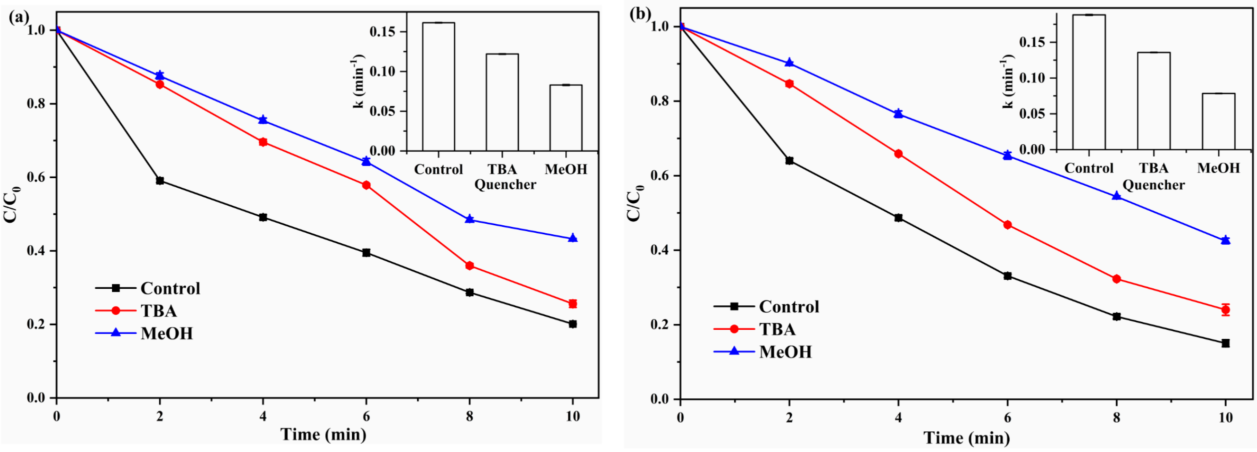

Figure 8. SFD degradation with quenchers. (**a**) Ozone/PS reaction system. (**b**) Ozone/PMS reaction system. Experiment conditions: [SFD] = 0.03 mM, [ozone flow rate] = 2.14 g/min, [PS] = 3.0 mM, [PMS] = 3.0 mM, [TBA] = 0.5 M, [MeOH] = 0.5 M.

2.7. Proposed Degradation Products and Pathways

The degradation products of SFD in the two reaction processes with ozone/PS and ozone/PMS were investigated, respectively. Three degradation products including C_{267}, C_{214} and C_{186} were detected from SFD degradation in the ozone/PS process. C_{267} at 268.03 m/z was formed from the attack of •OH on the benzene ring as well as the amino group on the benzene ring from the parent compound SFD. The opening of the pyrimidine ring resulted in C_{214} with an m/z value of 215.81. The SO_2 extrusion of SFD led to the generation of the compound 4-(2-iminopyrimidin-1(2H)-yl) aniline (C_{186}) with an m/z value of 187.85. C_{186} was also detected during SFD degradation under processes with MoS_2-Fe(III)-PMS, COF/PMS, S-Fe^0/PMS and so on [50,77,78]. According to the structures of the products, the transformation pathways including hydroxylation, the opening of the pyrimidine ring and SO_2 extrusion are revealed in Figure 9a.

Two intermediates—C_{267} and C_{180}—were detected during SFD degradation under the treatment process using ozone/PMS. C_{267} was the common degradation product of SFD in the two reactions with ozone/PS and ozone/PMS. C_{180} with an m/z value of 181.87 was generated from the opening of the pyrimidine ring and further oxidation. Though there was only one common product (C_{267}) in the two reactions, the degradation pathways were similar. Hydroxylation, pyrimidine ring opening and further oxidation are revealed in Figure 9b as the degradation pathways of SFD under the process with ozone/PMS.

Since neither the ozone/PS process nor the ozone/PMS process completely mineralized SFD, further understanding of the toxicity of SFD and its degradation intermediates is necessary. C_{214}, C_{186} and C_{180} were detected in the EA-PMS-MMO/MMO system for the degradation of SFD. Among them, C_{186} was more toxic to fish, Daphnia and green algae than SFD, while C_{214} and C_{180} were significantly less toxic than SFD [79]. Furthermore, the toxicity of C_{186} detected in the degradation of SFD by the S-Fe^0/PMS system was significantly higher than that of SFD [50]. This suggests that although the ozone/PS and ozone/PMS processes can degrade SFD effectively, the potential ecological risk of their degradation intermediates should not be ignored.

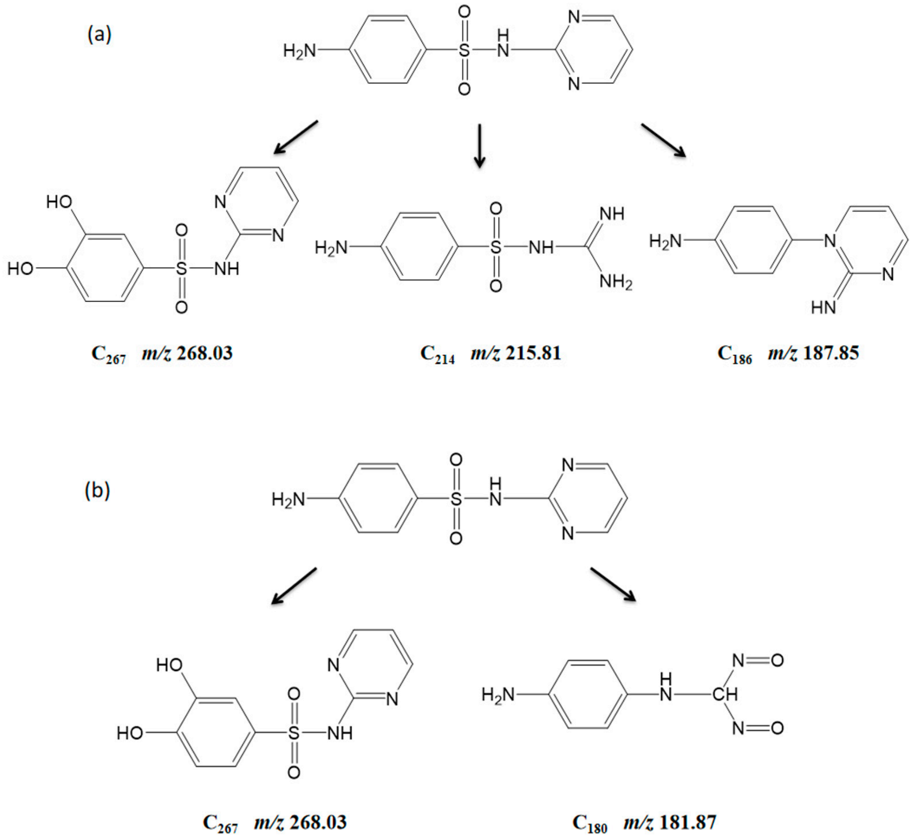

Figure 9. Degradation products and pathways of SFD. (**a**) Ozone/PS reaction. (**b**) Ozone/PMS reaction. Experiment conditions: [SFD] = 0.03 mM, [ozone flow rate] = 3.21 g/min, [PS] = 3.0 mM, [PMS] = 3.0 mM.

3. Methodology

3.1. Chemicals and Reagents

All the chemicals used in this study were purchased from Sigma-Aldrich (St. Louis, MO, USA). The chemicals used in the reactions were of at least analytical standard, and the solvents employed in HPLC and LC/MS analyses were of HPLC grade and LC/MS grade, respectively. All solutions were prepared in ultrapure water from a Barnstead NANO pure water system (Thermo Fisher Scientific Inc., Waltham, MA, USA). The nitrogen supplied by Zhuhai Huateya industrial gas Co., LTD. (Zhuhai, China) with a purity higher than 99.999% was employed in IC analysis. Table 2 shows information regarding the chemicals used in this study. The oxygen with a purity higher than 99.7%, supplied by Linde HKO Ltd. (Hong Kong, China), was used for ozone generation as well as TOC analysis.

Table 2. Information of chemicals used in this study.

Name	CAS No.	Molecular Weight	Formula	Purity	Manufacturer
Target compounds					
Sulfadiazine (SFD)	68-35-9	250.28	$C_{10}H_{10}N_4O_2S$	99.0%	Sigma Aldrich Inc.
Compounds used in HPLC and LC/MS analyses					
Acetonitrile	75-05-8	41.05	C_2H_3N	≥99.9%	Sigma Aldrich Inc.
Potassium phosphate	7778-77-0	136.09	KH_2PO_4	≥99.5%	Sigma Aldrich Inc.
Formic acid	64-18-6	46.03	CH_2O_2	≥98.0%	Sigma Aldrich Inc.

Table 2. *Cont.*

Name	CAS No.	Molecular Weight	Formula	Purity	Manufacturer
		Compounds used for degradation experiments			
Hydrochloric acid	7647-01-0	36.46	HCl	≥96.0%	Sigma Aldrich Inc.
Sodium hydroxide	1310-73-2	40.00	$NaOH$	≥97.0%	Sigma Aldrich Inc.
Peroxymonosulfate	37222-66-5	152.17	$KHSO_5 \cdot 0.\ 5KHSO_4 \cdot 0.5\ K_2SO_4$	>4.0% (active oxygen)	Sigma Aldrich Inc.
Persulfate	7727-21-1	270.02	$K_2S_2O_8$	≥99.0% (RT)	Sigma Aldrich Inc.
Sodium thiosulfate pentahydrate	10102-17-7	248.18	$Na_2S_2O_3 \cdot 5H_2O$	≥99.5%	Sigma Aldrich Inc.
Sodium nitrite	7632-00-0	69.00	$NaNO_2$	≥97.0%	Sigma Aldrich Inc.
Sodium nitrate	7631-99-4	84.99	$NaNO_3$	≥99.0%	Sigma Aldrich Inc.
Sodium chloride	7647-14-5	58.44	$NaCl$	≥99.5%	Sigma Aldrich Inc.
Sodium bromide	7647-15-6	102.89	$NaBr$	≥99.0%	Sigma Aldrich Inc.
Sodium sulfate	7757-82-6	142.04	Na_2SO_4	≥99.0%	Sigma Aldrich Inc.
Sodium phosphate	7601-54-9	163.94	Na_3PO_4	96%	Sigma Aldrich Inc.
Methanol	67-56-1	32.04	CH_4O	≥99.8%	Sigma Aldrich Inc.
Tert-Butanol	75-65-0	74.12	$C_4H_{10}O$	≥99.0%	Sigma Aldrich Inc.

3.2. Experimental Procedures

All experiments were conducted in duplicate at 22 ± 0.5 °C unless stated otherwise. SFD degradation experiments were performed in a 500 mL gas washing bottle. The experimental setup is shown in Figure 10. Ozone was generated from the ozone generator (Model 2001, Jelight, Irvine, CA, USA) and diffused from the catheter. The experimental procedure was as follows: The reaction was started by turning on the switch for ozone entry and adding a certain amount (1.5–15 mL) of PS or PMS (0.1 M) simultaneously. The selection of [SDZ], [PS] and [PMS] concentrations; ozone flow; and pH comprised the preliminary studies of the research group. In addition, the literature provided references for initial parameter selection, including the efficient degradation of chloramphenicol, sulfamethoxazole and sulfadiazine by O_3/PMS, O_3/PS and MBR/O_3 processes, respectively [42,43,80]. The initial pH of the reaction solution was adjusted using HCl (1 M) and NaOH (1 M). At the preset intervals, samples were collected and overdosed $Na_2S_2O_3$ was added to terminate the reaction. The wastewater effluent was collected from Tai Po Sewage Treatment Plant in Hong Kong, and the property of the effluent is shown in Table 3. The pH value of the effluent was determined with a pH meter (pH/ION 735, ionLab). The concentrations of inorganic ions in the wastewater sample were determined using ion chromatography (IC, Thermo Scientific (Waltham, MA, USA), https://www.thermofisher.cn/order/catalog/product/22176-60004?ICID=search-product (accessed on 3 July 2023).

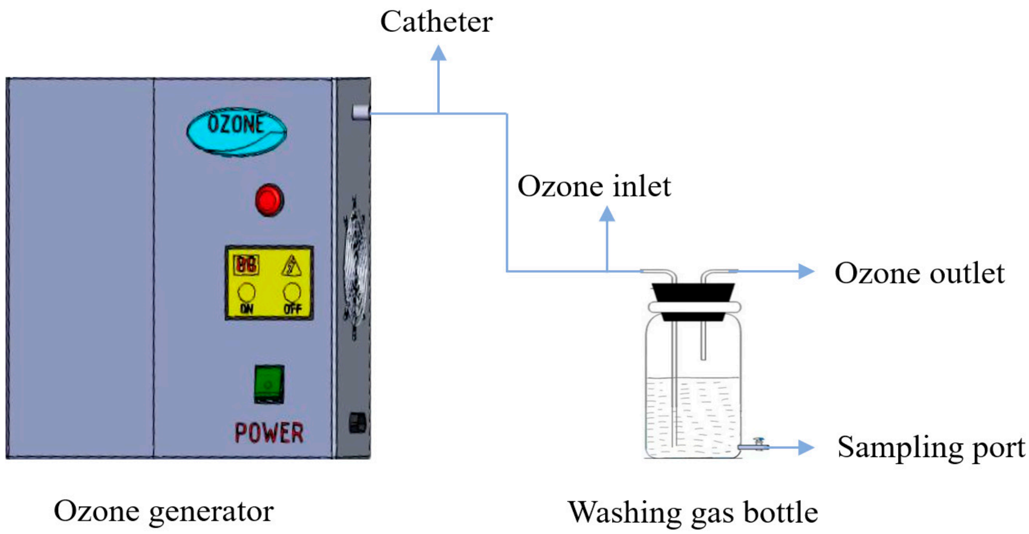

Figure 10. The experimental setup for SFD degradation.

Table 3. Property of the effluent.

Parameter	Value	Parameter	Value
pH	6.55	$[Cu^{2+}]$ (mg/L)	0.019
$[PO_4^{3-}]$ (mg/L)	2	$[Zn^{2+}]$ (mg/L)	0.05
$[SO_4^{2-}]$ (mg/L)	567.9	$[Mg^{2+}]$ (mg/L)	>149.171
$[Br^-]$ (mg/L)	13.3	$[Sr^{2+}]$ (mg/L)	0.976
$[Cl^-]$ (mg/L)	3750	$[Ca^{2+}]$ (mg/L)	66.986
$[NO_3^-]$ (mg/L)	0.127	$[Se^{2+}]$ (mg/L)	0.01
$[NO_2^-]$ (mg/L)	1.1	$[K^+]$ (mg/L)	>96.000

3.3. Analytic Methods

The residual SFD was detected by high-performance liquid chromatography (HPLC) with a Water 515 HPLC pump and 2487 detector. The mobile phase consisted of 50% acetonitrile (ACN) and 50% 10 mM KH_2PO_4 solution, and the pH was adjusted to 3 by adding an H_3PO_4 solution. The elution flow rate was set at 1 mL/min and the 10 µL sample was injected. The detection wavelength was set at 265 nm. The peak areas of SFD were recorded and the SFD concentrations were calculated accordingly. Total organic carbon (TOC) was measured by a TOC analyzer equipped with an autosampler (Shimadzu, ASI-L, Kyoto, Japan) and a CO_2 conductivity detector. The 680 °C combustion catalytic oxidation method was adopted in TOC analysis (https://www.shimadzu.com/an/products/total-organic-carbon-analysis/toc-analysis/toc-l-series/features.html#anchor_0, accessed on 3 July 2023). The samples underwent combustion through heating to 680 °C with a platinum catalyst and were converted to carbon dioxide, which was further detected using an infrared gas analyzer (NDIR).

A UPLC/ESI-MS system that consisted of a quaternary pump, an autosampler, a vacuum degasser, a thermostated column compartment and a diode array detector (DAD) coupled with an ion trap mass spectrometer detector (MSD) was used for the detection and analysis of the transformation byproducts. A Bruker amaZon SL ion trap mass analyzer (Bruker, Billerica, MA, USA) was used for the mass analysis in both positive and negative ion modes. Dionex UltiMate 3000 (Dionex, Sunnyvale, CA, USA) Ultra-high Performance Liquid Chromatography (UPLC) was carried out to obtain the chromatography. The UPLC was equipped with a Thermo Hypersil GOLD column (1.9 µm, 50 × 2.1 mm) (Waltham, MA, USA). The temperature of the column was kept at 30 °C during the analysis. The flow rate of the mobile phase was 0.15 mL/min and the injection volume of the samples was 5 µL. Acetonitrile and 0.1% formic acid were used as the mobile phases, which were marked as A and B solutions, respectively. The gradient washing was progressed from 10% A (0–2 min) to 60% A in 2–15 min linearly, maintained at 60% A for 3 min, and finally went back to 10% A. The system was controlled by the LC/MSD ChemStation (Dayton, OH, USA) software version A.09.03. Isopropyl alcohol and 0.1% formic acid were used as the washing solvents. Nitrogen was employed as a nebulizer as well as a drying gas.

4. Conclusions

This study focused on the degradation, mineralization and reaction mechanism of SFD by ozone/PS and ozone/PMS processes. The ozone/PMS and ozone/PS processes promoted the degradation of SFD compared to processes with sole ozone, sole PMS and sole PS. The results of quenching experiments showed that •OH and $SO_4\bullet^-$ radicals contributed to SFD elimination in the ozone/PS and ozone/PMS processes and $SO_4\bullet^-$ played a relatively major role. In addition, the initial concentration of SFD, oxidant dosages, initial pH and inorganic anions influenced the degradation of SFD. A higher oxidant dosage and lower initial SFD concentration resulted in a higher SFD removal reaction rate in the two ozone-based catalysis processes. For the ozone/PS process, the SFD removal rate increased with increasing solution pH, with an optimum pH of approximately 9.5. The anions PO_4^{3-}, NO_3^- and NO_2^- inhibited the removal of SFD by ozone/PS, while SO_4^{2-}, Br^- and Cl^- enhanced the removal of SFD. In the ozone/PMS process, the initial pH in the range of 3.5 to 9.5 showed an insignificant effect on the degradation of SFD. PO_4^{3-}, NO_3^-, NO_2^-, SO_4^{2-}, Br^- and Cl^- showed positive effects on the removal of SFD. In the ultrapure water and wastewater effluents, the degradation efficiency of SFD by different processes was in the order of ozone/PMS > ozone/PS > ozone. TOC removal in wastewater effluent was higher than that in ultrapure water in the two ozone-based catalysis processes. Under the treatment process ozone/PS, the degradation pathways of SFD included hydroxylation, the opening of the pyrimidine ring and SO_2 extrusion, while hydroxylation, pyrimidine ring opening and further oxidation were the main degradation pathways under the treatment process with ozone/PMS. This work confirms that the two ozone-based catalysis processes are efficient methods for the treatment of antibiotics from wastewater effluents.

Author Contributions: R.L.: Investigation, experimental, data analysis, writing—original draft preparation. Y.Z.: Investigation, data analysis, writing—original draft preparation. F.L. (Fengru Lu): Data analysis, writing—original draft preparation. F.L. (Feng Li): Writing. L.X.: Data analysis, investigation. L.G.: Data analysis. C.C.: Data analysis, resource curation. X.L.: Investigation. Q.J.: Experiments. W.C.: Supervision. M.Y.: Data analysis, supervision. H.G.: Supervision, funding acquisition, project administration, data analysis. All authors have read and agreed to the published version of the manuscript.

Funding: This work was supported by the National Natural Science Foundation of China (41807476) and the Guangzhou Science and Technology Project (Basic and Applied Basic Research project, 202102020892).

Conflicts of Interest: The authors declare no conflict of interest. The authors declare that they have no known competing financial interests or personal relationships that could have appeared to influence the work reported in this paper.

References

1. Deniere, E.; Van Langenhove, H.; Van Hulle, S.W.H.; Demeestere, K. Improving the ozone-activated peroxymonosulfate process for removal of trace organic contaminants in real waters through implementation of an optimized sequential ozone dosing strategy. *Sci. Total Environ.* **2023**, *856*, 158764. [CrossRef]
2. Deniere, E.; Van Langenhove, H.; Van Hulle, S.; Demeestere, K. The ozone-activated peroxymonosulfate process for the removal of a mixture of TrOCs with different ozone reactivity at environmentally relevant conditions: Technical performance, radical exposure and online monitoring by spectral surrogate parameters. *Chem. Eng. J.* **2023**, *454*, 140128. [CrossRef]
3. Deniere, E.; Alagappan, R.P.; Langenhove, H.V.; Hulle, S.V.; Demeestere, K. The ozone-activated peroxymonosulfate process (O_3/PMS) for removal of trace organic contaminants in natural and wastewater: Effect of the (in)organic matrix composition. *Chem. Eng. J.* **2022**, *430*, 133000. [CrossRef]
4. Tian, Y.; Yao, S.; Zhou, L.; Hu, Y.; Lei, J.; Wang, L.; Zhang, J.; Liu, Y.; Cui, C. Efficient removal of antibiotic-resistant bacteria and intracellular antibiotic resistance genes by heterogeneous activation of peroxymonosulfate on hierarchical macro-mesoporous Co_3O_4-SiO_2 with enhanced photogenerated charges. *J. Hazard. Mater.* **2022**, *430*, 127414. [CrossRef] [PubMed]
5. Ma, Y.; Wang, Z.; Yang, W.; Chen, C.; Li, J.; He, R.; Liu, S. Insights into the radical and nonradical oxidation degradation of ciprofloxacin in peroxodisulfate activation by ultraviolet light. *J. Water Process Eng.* **2022**, *49*, 103184. [CrossRef]
6. Zhou, C.S.; Wu, J.W.; Dong, L.L.; Liu, B.F.; Xing, D.F.; Yang, S.S.; Wu, X.K.; Wang, Q.; Fan, J.N.; Feng, L.P.; et al. Removal of antibiotic resistant bacteria and antibiotic resistance genes in wastewater effluent by UV-activated persulfate. *J. Hazard. Mater.* **2020**, *388*, 122070. [CrossRef]
7. Giannakis, S.; Le, T.M.; Entenza, J.M.; Pulgarin, C. Solar photo-Fenton disinfection of 11 antibiotic-resistant bacteria (ARB) and elimination of representative AR genes. Evidence that antibiotic resistance does not imply resistance to oxidative treatment. *Water Res.* **2018**, *143*, 334–345. [CrossRef]
8. Modak, S.M.; Sampath, L.; Fox, C.L., Jr. Combined topical use of silver sulfadiazine and antibiotics as a possible solution to bacterial resistance in burn wounds. *J. Burn Care Rehabil.* **1988**, *9*, 359–363. [CrossRef] [PubMed]
9. Schauss, K.; Focks, A.; Heuer, H.; Kotzerke, A.; Schmitt, H.; Thiele-Bruhn, S.; Smalla, K.; Wilke, B.-M.; Matthies, M.; Amelung, W.; et al. Analysis, fate and effects of the antibiotic sulfadiazine in soil ecosystems. *TrAC Trends Anal. Chem.* **2009**, *28*, 612–618. [CrossRef]
10. Schauss, K.; Focks, A.; Leininger, S.; Kotzerke, A.; Heuer, H.; Thiele-Bruhn, S.; Sharma, S.; Wilke, B.M.; Matthies, M.; Smalla, K.; et al. Dynamics and functional relevance of ammonia-oxidizing archaea in two agricultural soils. *Environ. Microbiol.* **2009**, *11*, 446–456. [CrossRef]
11. Miao, X.-S.; Bishay, F.; Chen, M.; Metcalfe, C.D. Occurrence of Antimicrobials in the Final Effluents of Wastewater Treatment Plants in Canada. *Environ. Sci. Technol.* **2004**, *38*, 3533–3541. [CrossRef]
12. Qin, L.T.; Pang, X.R.; Zeng, H.H.; Liang, Y.P.; Mo, L.Y.; Wang, D.Q.; Dai, J.F. Ecological and human health risk of sulfonamides in surface water and groundwater of Huixian karst wetland in Guilin, China. *Sci. Total Environ.* **2020**, *708*, 134552. [CrossRef]

13. de Orte, M.R.; Carballeira, C.; Viana, I.G.; Carballeira, A. Assessing the toxicity of chemical compounds associated with marine land-based fish farms: The use of mini-scale microalgal toxicity tests. *Chem. Ecol.* **2013**, *29*, 554–563. [CrossRef]
14. Lin, T.; Chen, Y.; Chen, W. Impact of toxicological properties of sulfonamides on the growth of zebrafish embryos in the water. *Environ. Toxicol. Pharmacol.* **2013**, *36*, 1068–1076. [CrossRef]
15. Wollenberger, L.; Halling-Sørensen, B.; Kusk, K.O. Acute and chronic toxicity of veterinary antibiotics to Daphnia magna. *Chemosphere* **2000**, *40*, 723–730. [CrossRef] [PubMed]
16. Xu, R.; Qian, K.; Xie, X.; Chen, J.; Tang, W.; Tao, F.; Wang, Y. In situ degradation of fluoroquinolone antibiotics in groundwater by $CoFe_2O_4$ nanoparticle-activated peroxymonosulfate: Performance, activation mechanism, degradation pathway. *Appl. Geochem.* **2023**, *152*, 105605. [CrossRef]
17. Chen, X.; Chen, J.; Yu, X.; Sanganyado, E.; Wang, L.; Li, P.; Liu, W. Effects of norfloxacin, copper, and their interactions on microbial communities in estuarine sediment. *Environ. Res.* **2022**, *212*, 113506. [CrossRef]
18. Castrignano, E.; Yang, Z.; Feil, E.J.; Bade, R.; Castiglioni, S.; Causanilles, A.; Gracia-Lor, E.; Hernandez, F.; Plosz, B.G.; Ramin, P.; et al. Enantiomeric profiling of quinolones and quinolones resistance gene qnrS in European wastewaters. *Water Res.* **2020**, *175*, 115653. [CrossRef] [PubMed]
19. Zhang, X.; Su, H.; Gao, P.; Li, B.; Feng, L.; Liu, Y.; Du, Z.; Zhang, L. Effects and mechanisms of aged polystyrene microplastics on the photodegradation of sulfamethoxazole in water under simulated sunlight. *J. Hazard. Mater.* **2022**, *433*, 128813. [CrossRef] [PubMed]
20. Gulkowska, A.; Leung, H.W.; So, M.K.; Taniyasu, S.; Yamashita, N.; Yeung, L.W.; Richardson, B.J.; Lei, A.P.; Giesy, J.P.; Lam, P.K. Removal of antibiotics from wastewater by sewage treatment facilities in Hong Kong and Shenzhen, China. *Water Res.* **2008**, *42*, 395–403. [CrossRef]
21. Li, J.; Ren, S.; Qiu, X.; Zhao, S.; Wang, R.; Wang, Y. Electroactive ultrafiltration membrane for simultaneous removal of antibiotic, antibiotic resistant bacteria, and antibiotic resistance genes from wastewater effluent. *Environ. Sci. Technol.* **2022**, *56*, 15120–15129. [CrossRef] [PubMed]
22. Avramiotis, E.; Frontistis, Z.; Manariotis, I.D.; Vakros, J.; Mantzavinos, D. On the Performance of a Sustainable Rice Husk Biochar for the Activation of Persulfate and the Degradation of Antibiotics. *Catalysts* **2021**, *11*, 1303. [CrossRef]
23. Huang, H.; Jiang, L.; Yang, J.; Zhou, S.; Yuan, X.; Liang, J.; Wang, H.; Wang, H.; Bu, Y.; Li, H. Synthesis and modification of ultrathin g-C_3N_4 for photocatalytic energy and environmental applications. *Renew. Sust. Energy Rev.* **2023**, *173*, 113110. [CrossRef]
24. Jiang, L.; Zhou, S.; Yang, J.; Wang, H.; Yu, H.; Chen, H.; Zhao, Y.; Yuan, X.; Chu, W.; Li, H. Near-Infrared Light Responsive TiO_2 for Efficient Solar Energy Utilization. *Adv. Funct. Mater.* **2021**, *32*, 2108977. [CrossRef]
25. Li, H.; Zhang, Z.; Duan, J.; Li, N.; Li, B.; Song, T.; Sardar, M.F.; Lv, X.; Zhu, C. Electrochemical disinfection of secondary effluent from a wastewater treatment plant: Removal efficiency of ARGs and variation of antibiotic resistance in surviving bacteria. *Chem. Eng. J.* **2020**, *392*, 123674. [CrossRef]
26. Cui, C.; Jin, L.; Jiang, L.; Han, Q.; Lin, K.; Lu, S.; Zhang, D.; Cao, G. Removal of trace level amounts of twelve sulfonamides from drinking water by UV-activated peroxymonosulfate. *Sci. Total Environ.* **2016**, *572*, 244–251. [CrossRef] [PubMed]
27. Yan, J.; Travis, B.R.; Borhan, B. Direct Oxidative Cleavage of α- and β-Dicarbonyls and α-Hydroxyketones to Diesters with $KHSO_5$. *J. Org. Chem.* **2004**, *69*, 9299–9302. [CrossRef] [PubMed]
28. Liu, F.; Li, Z.; Dong, Q.; Nie, C.; Wang, S.; Zhang, B.; Han, P.; Tong, M. Catalyst-free periodate activation by solar irradiation for bacterial disinfection: Performance and mechanisms. *Environ. Sci. Technol.* **2022**, *56*, 4413–4424. [CrossRef] [PubMed]
29. Rivas, F.J.; Gimeno, O.; Borallho, T. Aqueous pharmaceutical compounds removal by potassium monopersulfate. Uncatalyzed and catalyzed semicontinuous experiments. *Chem. Eng. J.* **2012**, *192*, 326–333. [CrossRef]
30. Chu, L.; Zhuan, R.; Chen, D.; Wang, J.; Shen, Y. Degradation of macrolide antibiotic erythromycin and reduction of antimicrobial activity using persulfate activated by gamma radiation in different water matrices. *Chem. Eng. J.* **2019**, *361*, 156–166. [CrossRef]
31. How, Z.T.; Fang, Z.; Chelme-Ayala, P.; Ganiyu, S.O.; Zhang, X.; Xu, B.; Chen, C.; Gamal El-Din, M. Ozone-activated peroxymonosulfate (O_3/PMS) process for the removal of model naphthenic acids compounds: Kinetics, reactivity, and contribution of oxidative species. *J. Environ. Chem. Eng.* **2023**, *11*, 109935. [CrossRef]
32. Zawadzki, P.; Deska, M. Degradation Efficiency and Kinetics Analysis of an Advanced Oxidation Process Utilizing Ozone, Hydrogen Peroxide and Persulfate to Degrade the Dye Rhodamine B. *Catalysts* **2021**, *11*, 974. [CrossRef]
33. Yang, S.; Wang, P.; Yang, X.; Shan, L.; Zhang, W.; Shao, X.; Niu, R. Degradation efficiencies of azo dye Acid Orange 7 by the interaction of heat, UV and anions with common oxidants: Persulfate, peroxymonosulfate and hydrogen peroxide. *J. Hazard. Mater.* **2010**, *179*, 552–558. [CrossRef]
34. Gao, P.; Tian, X.; Nie, Y.; Yang, C.; Zhou, Z.; Wang, Y. Promoted peroxymonosulfate activation into singlet oxygen over perovskite for ofloxacin degradation by controlling the oxygen defect concentration. *Chem. Eng. J.* **2019**, *359*, 828–839. [CrossRef]
35. Zhang, Y.; Zhao, Y.-G.; Yang, D.; Zhao, Y. Insight into the removal of tetracycline-resistant bacteria and resistance genes from mariculture wastewater by ultraviolet/persulfate advanced oxidation process. *J. Hazard. Mater. Adv.* **2022**, *7*, 100129. [CrossRef]
36. Liu, Y.; Gao, J.; Wang, Y.; Duan, W.; Liu, J.; Zhang, Y.; Zhang, H.; Zhao, M. The removal of antibiotic resistant bacteria and genes and inhibition of the horizontal gene transfer by contrastive research on sulfidated nanoscale zerovalent iron activating peroxymonosulfate or peroxydisulfate. *J. Hazard. Mater.* **2022**, *423*, 126866. [CrossRef]
37. Yu, Z.; Rabiee, H.; Guo, J. Synergistic effect of sulfidated nano zerovalent iron and persulfate on inactivating antibiotic resistant bacteria and antibiotic resistance genes. *Water Res.* **2021**, *198*, 117141. [CrossRef]

38. Feng, M.; Cizmas, L.; Wang, Z.; Sharma, V.K. Synergistic effect of aqueous removal of fluoroquinolones by a combined use of peroxymonosulfate and ferrate(VI). *Chemosphere* **2017**, *177*, 144–148. [CrossRef]
39. Lange, F.; Cornelissen, S.; Kubac, D.; Sein, M.M.; von Sonntag, J.; Hannich, C.B.; Golloch, A.; Heipieper, H.J.; Moder, M.; von Sonntag, C. Degradation of macrolide antibiotics by ozone: A mechanistic case study with clarithromycin. *Chemosphere* **2006**, *65*, 17–23. [CrossRef]
40. Qiao, J.; Luo, S.; Yang, P.; Jiao, W.; Liu, Y. Degradation of Nitrobenzene-containing wastewater by ozone/persulfate oxidation process in a rotating packed bed. *J. Taiwan Inst. Chem. Eng.* **2019**, *99*, 1–8. [CrossRef]
41. Yang, J.; Li, Y.; Yang, Z.; Shih, K.; Ying, G.-G.; Feng, Y. Activation of ozone by peroxymonosulfate for selective degradation of 1,4-dioxane: Limited water matrices effects. *J. Hazard. Mater.* **2022**, *436*, 129223. [CrossRef] [PubMed]
42. Cao, Y.; Qiu, W.; Zhao, Y.; Li, J.; Jiang, J.; Yang, Y.; Pang, S.-Y.; Liu, G. The degradation of chloramphenicol by O_3/PMS and the impact of O_3-based AOPs pre-oxidation on dichloroacetamide generation in post-chlorination. *Chem. Eng. J.* **2020**, *401*, 126146. [CrossRef]
43. Adil, S.; Maryam, B.; Kim, E.J.; Dulova, N. Individual and simultaneous degradation of sulfamethoxazole and trimethoprim by ozone, ozone/hydrogen peroxide and ozone/persulfate processes: A comparative study. *Environ. Res.* **2020**, *189*, 109889. [CrossRef] [PubMed]
44. Wu, S.; Li, H.; Li, X.; He, H.; Yang, C. Performances and mechanisms of efficient degradation of atrazine using peroxymonosulfate and ferrate as oxidants. *Chem. Eng. J.* **2018**, *353*, 533–541. [CrossRef]
45. Zhai, G.; Liu, S.; Si, S.; Liu, Y.; Zhang, H.; Mao, Y.; Zhang, M.; Wang, Z.; Cheng, H.; Wang, P.; et al. Oxygen vacancies enhanced ozonation toward phenol derivatives removal over Ov-Bi_2O_3. *ACS EST Water* **2022**, *2*, 1725–1733. [CrossRef]
46. Zhou, X.; Yang, Z.; Chen, Y.; Feng, H.; Yu, J.; Tang, J.; Ren, X.; Tang, J.; Wang, J.; Tang, L. Single-atom Ru loaded on layered double hydroxide catalyzes peroxymonosulfate for effective *E. coli* inactivation via a non-radical pathway: Efficiency and mechanism. *J. Hazard. Mater.* **2022**, *440*, 129720. [CrossRef]
47. Jiang, Z.-R.; Li, Y.; Zhou, Y.-X.; Liu, X.; Wang, C.; Lan, Y.; Li, Y. Co_3O_4-MnO_2 nanoparticles moored on biochar as a catalyst for activation of peroxymonosulfate to efficiently degrade sulfonamide antibiotics. *Sep. Purif. Technol.* **2022**, *281*, 119935. [CrossRef]
48. Zou, Y.; Hu, J.; Li, B.; Lin, L.; Li, Y.; Liu, F.; Li, X.-Y. Tailoring the coordination environment of cobalt in a single-atom catalyst through phosphorus doping for enhanced activation of peroxymonosulfate and thus efficient degradation of sulfadiazine. *Appl. Catal. B Environ.* **2022**, *312*, 121408. [CrossRef]
49. Wang, T.; Lu, J.; Lei, J.; Zhou, Y.; Zhao, H.; Chen, X.; Faysal Hossain, M.; Zhou, Y. Highly efficient activation of peroxymonosulfate for rapid sulfadiazine degradation by $Fe_3O_4@Co_3S_4$. *Sep. Purif. Technol.* **2023**, *307*, 122755. [CrossRef]
50. Ling, C.; Wu, S.; Dong, T.; Dong, H.; Wang, Z.; Pan, Y.; Han, J. Sulfadiazine removal by peroxymonosulfate activation with sulfide-modified microscale zero-valent iron: Major radicals, the role of sulfur species, and particle size effect. *J. Hazard. Mater.* **2022**, *423*, 127082. [CrossRef]
51. Dong, F.-X.; Yan, L.; Huang, S.-T.; Liang, J.-Y.; Zhang, W.-X.; Yao, X.-W.; Chen, X.; Qian, W.; Guo, P.-R.; Kong, L.-J.; et al. Removal of antibiotics sulfadiazine by a biochar based material activated persulfate oxidation system: Performance, products and mechanism. *Process Saf. Environ. Prot.* **2022**, *157*, 411–419. [CrossRef]
52. Cui, H.; Tian, Y.; Zhang, J.; Ma, S.; Li, L.; Zuo, W.; Zhang, L.; Wang, T. Enhanced oxidation of sulfadiazine by two-stage ultrasound assisted zero-valent iron catalyzed persulfate process: Factors and pathways. *Chem. Eng. J.* **2021**, *417*, 128152. [CrossRef]
53. Chen, J.; Dai, C.; Zhu, Y.; Gao, Y.; Chu, W.; Gao, N.; Wang, Q. Degradation of sulfadiazine by UV/Oxone: Roles of reactive oxidative species and the formation of disinfection byproducts. *Environ. Sci. Pollut. Res. Int.* **2022**, *29*, 54407–54420. [CrossRef] [PubMed]
54. Gong, H.; Chu, W.; Huang, Y.; Xu, L.; Chen, M.; Yan, M. Solar photocatalytic degradation of ibuprofen with a magnetic catalyst: Effects of parameters, efficiency in effluent, mechanism and toxicity evolution. *Environ. Pollut.* **2021**, *276*, 116691. [CrossRef] [PubMed]
55. Cheng, X.; Guo, H.; Zhang, Y.; Wu, X.; Liu, Y. Non-photochemical production of singlet oxygen via activation of persulfate by carbon nanotubes. *Water Res.* **2017**, *113*, 80–88. [CrossRef] [PubMed]
56. Wu, L.; Lin, Q.; Fu, H.; Luo, H.; Zhong, Q.; Li, J.; Chen, Y. Role of sulfide-modified nanoscale zero-valent iron on carbon nanotubes in nonradical activation of peroxydisulfate. *J. Hazard. Mater.* **2022**, *422*, 126949. [CrossRef] [PubMed]
57. Deniere, E.; Van Hulle, S.; Van Langenhove, H.; Demeestere, K. Advanced oxidation of pharmaceuticals by the ozone-activated peroxymonosulfate process: The role of different oxidative species. *J. Hazard. Mater.* **2018**, *360*, 204–213. [CrossRef]
58. Chen, Y.; Bai, X.; Ji, Y.; Chen, D. Enhanced activation of peroxymonosulfate using ternary MOFs-derived MnCoFeO for sulfamethoxazole degradation: Role of oxygen vacancies. *J. Hazard. Mater.* **2023**, *441*, 129912. [CrossRef]
59. Mao, Y.; Dong, H.; Liu, S.; Zhang, L.; Qiang, Z. Accelerated oxidation of iopamidol by ozone/peroxymonosulfate (O_3/PMS) process: Kinetics, mechanism, and simultaneous reduction of iodinated disinfection by-product formation potential. *Water Res.* **2020**, *173*, 115615. [CrossRef]
60. Yang, Y.; Jiang, J.; Lu, X.; Ma, J.; Liu, Y. Production of sulfate radical and hydroxyl radical by reaction of ozone with peroxymonosulfate: A novel advanced oxidation process. *Environ. Sci. Technol.* **2015**, *49*, 7330–7339. [CrossRef]
61. Wang, X.-X.; Lin, Y.-L.; Zhang, T.-Y.; Dong, Z.-Y.; Luo, Z.-N.; Hu, C.-Y.; Tang, Y.-L.; Xu, B. Feasibility of UVC laser-activated persulfate with concentrated beam for micropollutant degradation in water. *Sep. Purif. Technol.* **2022**, *299*, 121598. [CrossRef]
62. Furman, O.S.; Teel, A.L.; Watts, R.J. Mechanism of base activation of persulfate. *Environ. Sci. Technol.* **2010**, *44*, 6423–6428. [CrossRef] [PubMed]
63. Zhao, L.; Hou, H.; Fujii, A.; Hosomi, M.; Li, F. Degradation of 1,4-dioxane in water with heat- and Fe^{2+}-activated persulfate oxidation. *Environ. Sci. Pollut. Res. Int.* **2014**, *21*, 7457–7465. [CrossRef]

64. Hayat, W.; Zhang, Y.; Huang, S.; Hussain, I.; Huang, R. Insight into the degradation of methomyl in water by peroxymonosulfate. *J. Environ. Chem. Eng.* **2021**, *9*, 105358. [CrossRef]
65. Wang, H.; Wu, Y.; Feng, M.; Tu, W.; Xiao, T.; Xiong, T.; Ang, H.; Yuan, X.; Chew, J.W. Visible-light-driven removal of tetracycline antibiotics and reclamation of hydrogen energy from natural water matrices and wastewater by polymeric carbon nitride foam. *Water Res.* **2018**, *144*, 215–225. [CrossRef] [PubMed]
66. Sanchez-Polo, M.; Lopez-Penalver, J.; Prados-Joya, G.; Ferro-Garcia, M.A.; Rivera-Utrilla, J. Gamma irradiation of pharmaceutical compounds, nitroimidazoles, as a new alternative for water treatment. *Water Res.* **2009**, *43*, 4028–4036. [CrossRef]
67. Wang, F.; Wang, W.; Yuan, S.; Wang, W.; Hu, Z.-H. Comparison of UV/H_2O_2 and UV/PS processes for the degradation of thiamphenicol in aqueous solution. *J. Photochem. Photobiol. A* **2017**, *348*, 79–88. [CrossRef]
68. Zhang, X.; Zhu, X.; Li, H.; Wang, C.; Zhang, T. Combination of peroxymonosulfate and Fe(VI) for enhanced degradation of sulfamethoxazole: The overlooked roles of high-valent iron species. *Chem. Eng. J.* **2023**, *453*, 139742. [CrossRef]
69. Zhang, Y.; Li, L.; Pan, Z.; Zhu, Y.; Shao, Y.; Wang, Y.; Yu, K. Degradation of sulfamethoxazole by UV/persulfate in different water samples: Influential factors, transformation products and toxicity. *Chem. Eng. J.* **2020**, *379*, 122354. [CrossRef]
70. Ghanbari, F.; Khatebasreh, M.; Mahdavianpour, M.; Lin, K.A. Oxidative removal of benzotriazole using peroxymonosulfate/ozone/ultrasound: Synergy, optimization, degradation intermediates and utilizing for real wastewater. *Chemosphere* **2020**, *244*, 125326. [CrossRef]
71. Jaafarzadeh, N.; Ghanbari, F.; Ahmadi, M. Efficient degradation of 2,4-dichlorophenoxyacetic acid by peroxymonosulfate/magnetic copper ferrite nanoparticles/ozone: A novel combination of advanced oxidation processes. *Chem. Eng. J.* **2017**, *320*, 436–447. [CrossRef]
72. Jorfi, S.; Kakavandi, B.; Motlagh, H.R.; Ahmadi, M.; Jaafarzadeh, N. A novel combination of oxidative degradation for benzotriazole removal using TiO_2 loaded on $Fe^{II}Fe_2{}^{III}O_4$@C as an efficient activator of peroxymonosulfate. *Appl. Catal. B Environ.* **2017**, *219*, 216–230. [CrossRef]
73. Klu, P.K.; Zhang, H.; Nasir Khan, M.A.; Wang, C.; Qi, J.; Sun, X.; Li, J. TiO_2/C coated Co_3O_4 nanocages for peroxymonosulfate activation towards efficient degradation of organic pollutants. *Chemosphere* **2022**, *308*, 136255. [CrossRef]
74. Wang, Y.; Cao, D.; Zhao, X. Heterogeneous degradation of refractory pollutants by peroxymonosulfate activated by CoO_x-doped ordered mesoporous carbon. *Chem. Eng. J.* **2017**, *328*, 1112–1121. [CrossRef]
75. Zhou, Y.; Jiang, J.; Gao, Y.; Pang, S.Y.; Ma, J.; Duan, J.; Guo, Q.; Li, J.; Yang, Y. Oxidation of steroid estrogens by peroxymonosulfate (PMS) and effect of bromide and chloride ions: Kinetics, products, and modeling. *Water Res.* **2018**, *138*, 56–66. [CrossRef]
76. Gábor, L.; József, K.; Zsuzsa, B.; Alíz, K.; Ildikó, K.; Dávid, B.; Marcell, T.; Lilla, V.; Fábián, I. One-versus two-electron oxidation with peroxomonosulfate ion reactions with iron(II), vanadium(IV), halide ions, and photoreaction with cerium(III). *Inorg. Chem.* **2009**, *48*, 1763–1773.
77. Li, Y.; Feng, Y.; Yang, B.; Yang, Z.; Shih, K. Activation of peroxymonosulfate by molybdenum disulfide-mediated traces of Fe(III) for sulfadiazine degradation. *Chemosphere* **2021**, *283*, 131212. [CrossRef] [PubMed]
78. Wang, B.; He, D.; Zhu, D.; Lu, Y.; Li, C.; Li, X.; Dong, S.; Lyu, C. Electron-rich ketone-based covalent organic frameworks supported nickel oxyhydroxide for highly efficient peroxymonosulfate activation and sulfadiazine removal: Performance and multi-path reaction mechanisms. *Sep. Purif. Technol.* **2022**, *296*, 121350. [CrossRef]
79. Yao, J.; Dong, Z.; Ye, X.; Yang, J.; Jia, Y.; Zhang, Y.; Liu, H. Electrochemically activated peroxymonosulfate with mixed metal oxide electrodes for sulfadiazine degradation: Mechanism, DFT study and toxicity evaluation. *Chemosphere* **2022**, *309*, 136695. [CrossRef]
80. Lastre-Acosta, A.M.; Palharim, P.H.; Barbosa, I.M.; Mierzwa, J.C.; Silva Costa Teixeira, A.C. Removal of sulfadiazine from simulated industrial wastewater by a membrane bioreactor and ozonation. *J. Environ. Manag.* **2020**, *271*, 111040. [CrossRef]